JACS
JOURNAL OF THE AMERICAN CHEMICAL SOCIETY
Article
Cite This: J. Am. Chem. Soc. 2019, 141, 15040−15045
pubs.acs.org/JACS

Room-Temperature Ferroelectricity in Group-IV Metal Chalcogenide Nanowires

Jun-Jie Zhang,[†,‡] Jie Guan,[‡] Shuai Dong,*[,‡] and Boris I. Yakobson*[,†,§]

[†]Department of Materials Science and NanoEngineering and [§]Department of Chemistry, Rice University, Houston, Texas 77005, United States

[‡]School of Physics, Southeast University, Nanjing 211189, China

Supporting Information

ABSTRACT: The realization of low-dimensional ferroelectrics is both fundamentally intriguing and practically appealing, to be used in nanoscale devices. Here, GeS and SnS nanowires are predicted to be one-dimensional (1D) ferroelectrics with inversion symmetry spontaneously broken by soft optical modes. Despite the low dimensionality, the estimated Curie point for GeS nanowires is above room temperature, benefiting experimental detection and suggesting realistic applications. To this end, further aspects of these 1D ferroelectrics are also examined, revealing the domain wall localization, switchable carrier mobility, and practically effective shieling by confining the nanowires inside the carbon nanotubes, all together potentially useful for nanoscale ferroelectric devices of broad interest.

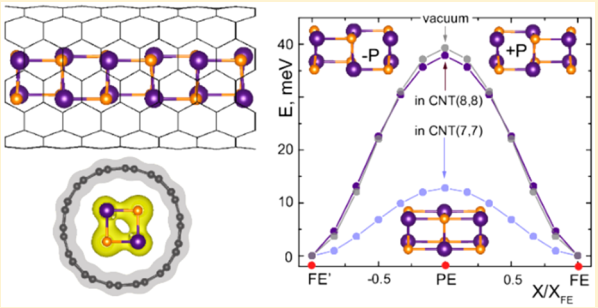

INTRODUCTION

Ferroelectrics, with spontaneous switchable electric polarization,[1] are a vital branch of functional materials due to their broad use in nanodevices, such as field-effect transistors (FET),[2] random-access memory (RAM),[3] and photovoltaics.[4,5] Nowadays, the miniaturization of ferroelectricity-based devices is suffering from the size limitation due to the internal depolarization field.[6−8] In order to overcome this challenge, significant progress has been made in two-dimensional (2D) ferroelectrics.[9−24] Differing from perovskite oxides, the ferroelectric polarization (P_{FE}) in 2D materials of atomic thickness can be strong enough to subsist, offering a natural solution for nanoscale ferroelectric applications.

However, while formally the extent of the remaining dimensions in 2D ferroelectrics is infinite, the in-plane ferroelectricity may be undercut by practical size reduction (as in ribbons or flakes). To circumvent this shortcoming, one-dimensional (1D) ferroelectrics with perfect "no-boundary" may provide a compelling alternative. Indeed, ferroelectricity has already been identified or proposed in quasi-1D systems of various chemistries,[25−31] such as tetrabromo-*p*-benzoquinone chain,[26] water molecules in quasi-1D beryl crystal,[29] $BaTiO_3$ and $PbTiO_3$ nanotubes,[30] and quasi-1D CsH_2PO_4.[31] However, these materials cannot be considered as really successful 1D ferroelectrics due to various issues, such as the difficulty of exfoliation into a stable 1D nanowire forms[31] or the large pore diameter (>10 nm) of perovskite nanotubes.[30] Desirable archetypal 1D ferroelectrics should be of nearly atom-small diameter, entailing also a structurally perfect "boundary", and of high stability, and such attributes still remain unavailable.

Recently, confinement inside carbon nanotubes (CNT) was shown as an efficient strategy of making not only monatomic chains of carbyne[32] but also nanowires of diverse chemical compositions.[33] In particular, 1D SnTe nanowires were experimentally synthesized inside the CNT,[34] with their crystal structure actually controlled by the CNT diameter: inside the narrow CNT the linear monatomic SnTe chain forms, while at larger CNT diameter the most favorable structure is a rocksalt-like SnTe nanowire; according calculations it retains its stability even outside CNT. Structurally, both the SnTe nanowire and the corresponding bulk phase are centrosymmetric. However, in other MX compositions (M = Ge, Sn and X = S, Se) in 2D or 3D more favorable is the black-phosphorus-like layered structure, where inversion symmetry is broken.[35] This suggests that monochalcogenide MX nanowires (formed in CNT) provide a likely route to pursue 1D ferroelectrics, aiming for high performance.

In the present work, we explore the ferroelectricity of SnS and GeS nanowires using density functional theory (DFT) computations, complemented by the fitted model analytics. The details of methods can be found in the Supporting Information (SI). On the basis of molecular dynamics (MD), the Curie temperature (T_C) of GeS nanowire is estimated to be above room temperature. Furthermore, somewhat practical issues of these 1D ferroelectrics are also investigated: the domain wall energy and spatial extent, the carrier mobility, as well as confinement of nanowires inside carbon nanotubes (as

Received: March 25, 2019
Published: September 4, 2019

DOI: 10.1021/jacs.9b03201
J. Am. Chem. Soc. 2019, 141, 15040−15045

seen for other similar 1D structures)—all to show their feasibility and promise for nanoscale ferroelectric devices of broad interest.

COMPUTATIONAL METHODS

The DFT calculations were performed using the Vienna ab initio simulation package (VASP).[36,37] The projector-augmented wave (PAW) potentials with the generalized gradient approximation of Perdew−Burke−Ernzerhof (GGA-PBE) formulation are used with a cutoff energy of 500 eV. A vacuum region with 20 Å thickness is introduced to eliminate interaction between nanowires, and the Brillouin zone is sampled with 1 × 1 × 20 *k*-points. More computational details can be found in the SI.

RESULTS AND DISCUSSION

A. Crystal Structure. Motivated by experimentally observed SnTe nanowires, we begin by constructing rocksalt-like SnS and GeS nanowires with nonpolar D_{4h} symmetry (paraelectric, PE), shown in Figure 1a. Unexpectedly, the

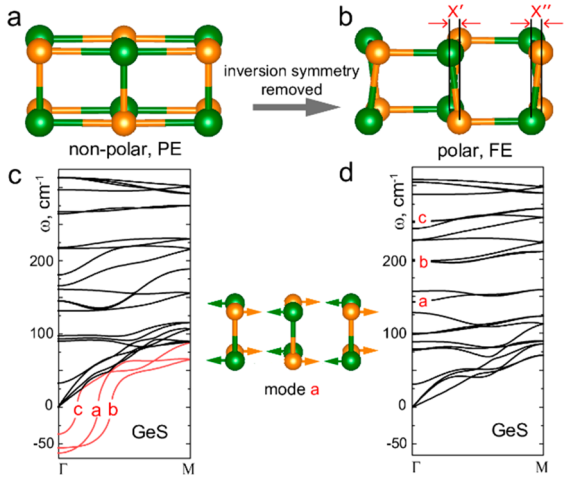

Figure 1. Structural phase transition in 1D MS. (a) Rocksalt-like structure; green and yellow are Ge and S atoms. (b) Its phonon dispersion, with unstable modes *a*, *b*, and *c* shown as red lines; the largest frequency most unstable is mode *a*. (c) Distorted polar 1D rocksalt-like GeS structure, and (d) its phonon dispersion; note all modes *a*, *b*, and *c*, now transformed into stable optical phonons.

structures appear dynamically unstable around Γ point in the phonon spectrum (Figure 1b for GeS and SI Figure S1a for SnS), where the imaginary-frequency modes must result in a shift of a cross-diagonal M atoms pair with respect to S atoms away from the centrosymmetric position, as characterized by X′ and X″ in Figure 1c. The mode *c* of largest imaginary frequency (ca. −62 cm^{-1} for GeS, ca. −71 cm^{-1} for SnS) corresponds to X′ = X″ = X in Figure 1c. This mode *c* breaks the space inversion symmetry and yields a structure of polar C_{4v} symmetry, Figure 1c. Note that now the phonon spectrum displays no imaginary frequencies, Figure 1d. (Two other imaginary-frequency modes are also noncentrosymmetric but would result in nonpolar structures of energy higher than the polar one, see Figure S1 and Table S1.)

To identify the most stable ferroelectric phase in 1D MS, including all soft modes a, b, and c (all being linear combinations of X′ and X″), the scanned free-energy contour is calculated with different values of X' and X''. Here, we again show GeS as an example, in Figure 2a. Two equivalent minima, separated by the nonpolar PE state ($X' = X'' = 0$), are found in

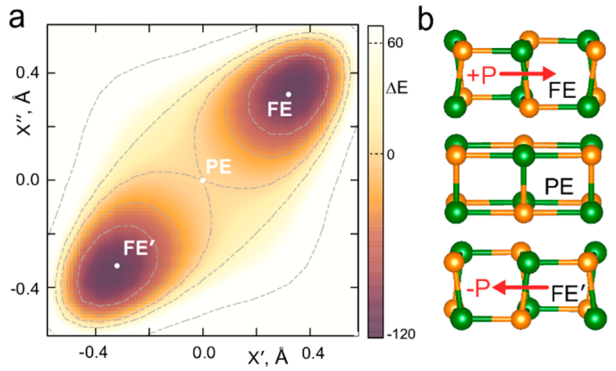

Figure 2. (a) Free-energy contour plot as a function of the Ge's displacements, X′ and X″; FE, FE′, and PE are marked. (b) Structures of FE, PE, and FE′ phase in 1D MS, FE, and FE′ have opposite polarization.

the diagonal direction, that is MS-nanowire prefers the $X' = X'' = \pm 0.4$ Å configuration. Thus, only pure *c*-mode distortion leads to the ground state, eliminating all imaginary frequencies. Importantly, these two minima in anharmonic double-well potential (along *X*) have opposite polarizations, labeled as FE and FE′ in Figure 2b, strongly suggesting the existence of ferroelectricity of 1D MS.

Before investigating the details of ferroelectricity in 1D SnS and GeS, the thermodynamic stability of ground-state structures should be evaluated by calculating their formation energies (using DFT+D2, with van der Waals correction, see SI in detail). With the energy of the bulk crystal as a reference (Table S2), the obtained values for FE 1D nanowires (~0.46 eV/fu for GeS, ~0.58 eV/fu for SnS) are slightly higher than for their corresponding 2D layers (~0.26 eV/fu for GeS, ~0.32 eV/fu for SnS) but lower than the energy of experimentally obtained 1D SnTe (~0.71 eV/fu above its bulk structure). Therefore, similar to rocksalt-like SnTe nanowire, it should be feasible to synthesize 1D SnS and GeS nanowires, perhaps in CNT of appropriate diameter.

B. Ferroelectricity. To characterize basic electronics, the calculated band structures of PE and FE of both SnS and GeS nanowires are shown in Figure S3; it is clear that they are all direct band-gap semiconductors with different band gaps (E_g), Table 1. We note that the band gap is not changed much if

Table 1. Calculated Band Gap E_g (eV), Atomic Displacement *X* (Å), Repolarization FE ↔ PE ↔ FE′ Barrier E_p (meV/cell), Polarization Quantum P_Q (10^{-10} C/m), and Spontaneous Polarization P_{FE} (10^{-10} C/m) of 1D GeS and SnS

	E_g	E_P	P_Q	*X*	P_{FE}
GeS	2.15(FE)/1.66(PE)	121.97	12.78	0.32	5.74
SnS	1.83(FE)/1.62(PE)	39.32	10.24	0.24	4.86

spin−orbit coupling is included, only some bands splitting around the Γ point (Figure S4). The finite band gap in the ferroelectric permits the switching of its polarization by applying an external electric field.

We then proceed to calculate the magnitude of such polarization following the ways of modern theory of polarization, especially using standard Berry phase calculations.[38,39] We take the PE structure as reference and select the side area of the nanowire unit cell to be able to compare with the values

DOI: 10.1021/jacs.9b03201
J. Am. Chem. Soc. 2019, 141, 15040−15045

for 2D layers of the same stoichiometry. This gives a significant spontaneous polarization of 5.7×10^{-10} C/m for GeS and 4.9×10^{-10} C/m for SnS, Figure 3a. Furthermore, the energy

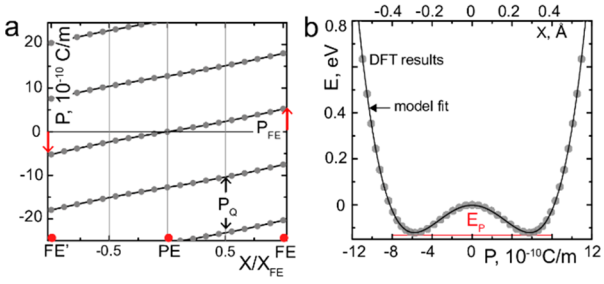

Figure 3. Ferroelectricity of GeS nanowire. (a) Polarization P as a function of atomic displacement, X. (b) Energy E as a function of P or X; repolarization barrier E_p is marked.

versus polarization P (or displacement X) is plotted in Figure 3b, where the anharmonic double-well energy curve is found to be in accord with ϕ^4 potential for ferroelectrics.[40] The large E_p = 122 meV (down from the PE state) in GeS indicates its strong ferroelectric instability, which is inherently related to the ferroelectric transition temperature. The value E_p = 39 meV for SnS is much smaller, implying its weaker ferroelectric instability.

It is a known concern that there should be no ferroelectric transition in 1D systems based on Landau theory.[41] A similar situation is also known in 1D isotropic magnetic systems, where long-range magnetic order is hardly achievable at nonzero temperature.[42] Even then there are two reasons alleviating this drawback of a low-dimensional system. First, it has been reported[43] that the interchain coupling can stabilize the long-range magnetic order in an array of infinite 1D wires (however, for optimized 1D MS ferroelectric, the interchain coupling favors antiparallel order, which is antiferroelectricity, see Table S3). Second, the prohibition is for the thermodynamic limit of the infinite, truly 1D systems. For MS nanowire of finite length, it is quite realistic to obtain the FE state at finite temperature, when the correlation length is beyond the length of nanowire.

In order to obtain this effective T_C, direct ab initio MD was employed for a 1D ferroelectric nanowire.[10−12,23,24] The MD results indicate that T_C is about 310 K for GeS, Figure 4a. With such T_C value above room temperature, the 1D FE nanowires appear attractive for applications. Due to the lower energy barrier of Ep in SnS nanowire, the corresponding $T_C \approx 230$ K is lower than that in GeS, Figure 4b. In addition, Monte Carlo

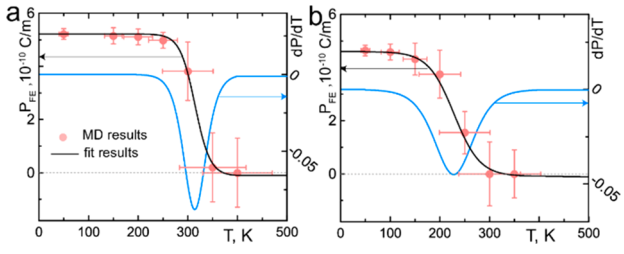

Figure 4. Temperature dependence of polarization obtained from ab initio molecular dynamics (red dots). Black lines are sigmoid fits to MD results and the pyroelectric response, dP/dT (blue line). (a) GeS and (b) SnS.

(MC) simulation based on polar mode a is also performed with the Landau−Ginzburg model,[40] as shown in SI (Section IV). The obtained T_C is much higher than the values from MD calculations, because MD simulation accounts for more phonon modes, which more realistically evaluates the energy barrier between ferroelectric and paraelectric phases at finite temperatures (nonpolar mode b may weaken the values of T_C during MD simulations).

Having now the values of spontaneous polarization P, the T_C, and the effects of finite temperature (via MD simulations), we can turn to the FE domain wall as a key for switching and domain spatial resolution for memory density. One can first estimate the domain wall width w (number of half-unit cells) by considering its energy cost using the following expression

$$E = \sum_i \frac{A}{2}(P_i)^2 + \frac{B}{2}(P_i)^4 + \frac{C}{2}\sum_{i,j}(P_i - P_j)^2 \quad (1)$$

where the first two terms express the energy contribution from the local modes up to the fourth order. The corresponding parameters A and B are obtained by fitting the double-well potential as shown in Figure 3b. The third term reflects the nearest-neighbor dipole−dipole coupling within nanowire, and the coefficient C is fitted by using mean-field theory within a nearest-neighbor approximation, Figure S6a. The obtained values of A, B, and C are listed in Table 2.

Table 2. Fitted to Match Direct DFT Data; A, B, and C Parameters of Eq 1[a]

	A	B	C	T_C
GeS	−14.4	0.22	7.31	310
SnS	−8.8	0.19	10.4	230

[a] T_C (K) is Curie temperature from MD calculations.

The polarization change across the wall from $-P$ to $+P$, by the increments of $\sim 2P/w$, brings about an extra energy $0.5 \cdot (A^2/8B) \cdot w + (AC/B) \cdot w^{-1}$. Its minimum is reached at $w \approx (C/A)^{1/2}$, which numerically yields $w \approx 3$ and 4 for GeS and SnS, respectively. Such a small value opportunely makes direct DFT computations affordable for a reasonably small segment, shown in Figure 5 after relaxation (as we tested, larger supercells do

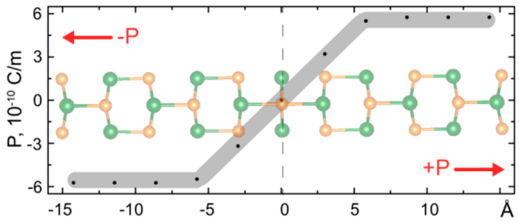

Figure 5. Domain wall structure in GeS and the FE P plot.

not change the wall structure, confirming the analytic estimate). The estimated energies of domain walls based on eq 1 are ~337 and ~146 meV for GeS and SnS and are in good agreement with DFT results (~376 meV for GeS, ~197 meV for SnS). The corresponding domain wall is very sharp, ~1 nm in Figure 5.

In experiments, by analogy with successful SnTe nanowires synthesis,[34] GeS or SnS wires should also be possible to produce inside CNT. Thus, the effect of CNT is also important to describe. Here, we take SnS as an example, due

DOI: 10.1021/jacs.9b03201
J. Am. Chem. Soc. 2019, 141, 15040−15045

to its lesser lattice mismatch with CNT (<2%). To simulate the experimental situation, an SnS nanowire is placed in the center of CNT of various diameters, Figure 6a. The formation

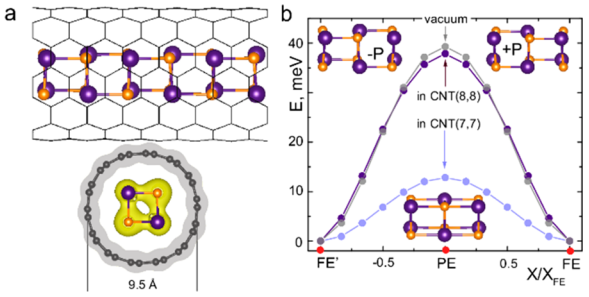

Figure 6. (a) (Top) Sketch of SnS nanowire in SWCNT; (bottom) computed charge density isosurface illustrates the radial fit of the wire. Purple and yellow are Sn and S atoms. (b) Energy change as a function of atom displacement X, in vacuum, inside (8,8) and (7,7) CNT.

(adsorption) energies for the SnS@CNT are calculated to be −0.71 and −1.99 eV/fu for (8,8) and (7,7) CNT, respectively. The repolarization energy barrier E_p is also decreased in smaller diameter CNT, Figure 6b, leading correspondingly to a lower Curie temperature. However, it does not change much the dipole moment, P_{FE}.

It is well known that the intrinsic electronic field in ferroelectric photovoltaic devices can effectively separate photoexcited electrons and holes, which is worthy to improve the photon-to-current efficiency.[4,5] Moreover, the carrier mobility is another important parameter for ferroelectric devices, which is proportional to conductivity in the semiconductor. Within the Boltzmann transport theory, their mobility is estimated by $\mu = \sigma/ne$,[44] where σ is the conductivity, n is the carrier density, and e is the elementary charge. To calculate σ, a constant carrier relaxation time τ is estimated using a phonon-limited scattering model.[45] Detailed descriptions about this method are provided in the Supporting Information.

The estimated $\tau \approx 10$ fs for GeS and SnS indicates the strong phonon scattering. In Figure 7 one can see that electron mobility (~180 $cm^2 V^{-1} s^{-1}$) is larger than hole mobility (~90 $cm^2 V^{-1} s^{-1}$) in GeS FE phase. If GeS changes from FE to PE, the mobility raises to ~160 $cm^2 V^{-1} s^{-1}$ for the holes, while it does not change much for electrons. However, the situation is much different in SnS where hole and electron mobilities are very similar in both FE (~125 $cm^2 V^{-1} s^{-1}$) and PE (~90 $cm^2 V^{-1} s^{-1}$) phases. Therefore, the carrier mobility in 1D MS is related tightly with polarization displacement X and can be switched by an external electric field.

It is noted that when 2D GeS and SnS are exfoliated from layered bulk phase there are no dangling bonds, and the ferroelectricy survives this process (in spite of some dangling bonds around the edges). Similarly, the ferroelectricy near the ends of 1D wires may be suppressed by unpaired ions around the ends (similar phenomena also exist for conventional 3D ferroelectrics due to their surfaces). Even though the ferroelectric distortion far from the ends should persist, the effect of end geometry on the ferroelectricity may be an interesting detail, which could be studied in further works.

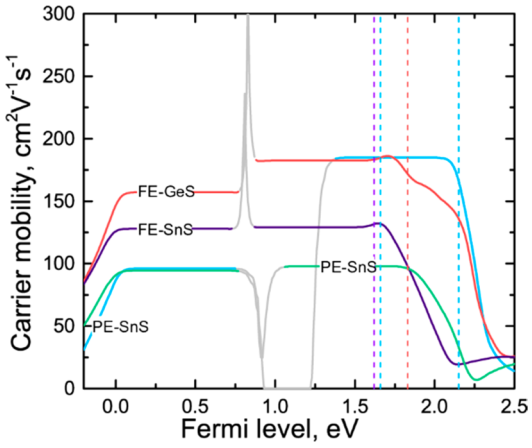

Figure 7. Calculated carrier mobility in 1D GeS and SnS. VBMs are set as zero; CBMs (conduction band minimum) of these systems are indicated by the vertical dashed line. Plateaus above the VBM stand for the hole mobility, while the plateaus below the CBM stand for the electron mobility. Note that the peaks near the middle of band gaps are caused by the too small and inaccurate carrier densities, which are not accurate or reliable and indicated by gray lines.

CONCLUSION

In summary, GeS and SnS nanowires, apparently synthetically feasible by analogy with already obtained SnTe, are predicted here to be quasi-1D ferroelectrics, with the Curie point reaching above room temperature in GeS nanowires. For the more likely experimental system of MS in CNT, the repolarization energy barrier and Curie temperature will be influenced by the adsorption to the encapsulating CNT. The wires display rather thin/abrupt domain walls of ~1 nm width, suggesting the possibility, in principle, of high density for memory functionality. The calculated carrier mobility shows tight connection with ferroelectric displacement X and can thus be switched by an external electric field. The stable and robust ferroelectricity in quasi-1D structures and their potential applications in nanoscale devices offer a very promising topic for future work.

ASSOCIATED CONTENT

Supporting Information

The Supporting Information is available free of charge on the ACS Publications website at DOI: 10.1021/jacs.9b03201.

Computational details; phonon dispersion of 1D GeS and SnS; formation energy and electronic structure of 1D GeS and SnS; more details of Monte Carlo simulations; more details of carrier mobility (PDF)

AUTHOR INFORMATION

Corresponding Authors

*sdong@seu.edu.cn
*biy@rice.edu

ORCID

Jun-Jie Zhang: 0000-0002-4779-2725
Shuai Dong: 0000-0002-6910-6319

Notes

The authors declare no competing financial interest.

DOI: 10.1021/jacs.9b03201
J. Am. Chem. Soc. 2019, 141, 15040−15045

■ ACKNOWLEDGMENTS

Work at Rice University was supported by the Robert Welch Foundation (C-1590) and, in CNT aspects, by the Air Force Office of Scientific Research (FA9550-14-1-0107). Work at Southeast University was supported by the National Natural Science Foundation of China (Grant Nos. 11834002, 11674055, and 61704110).

■ REFERENCES

(1) Lines, M. E.; Glass, A. M. *Principles and applications of ferroelectrics and related materials*; Oxford University Press, 2001.
(2) Naber, R. C.; Tanase, C.; Blom, P. W.; Gelinck, G. H.; Marsman, A. W.; Touwslager, F. J.; Setayesh, S.; De Leeuw, D. M. High-performance solution-processed polymer ferroelectric field-effect transistors. *Nat. Mater.* **2005**, *4* (3), 243.
(3) Scott, J. Data storage: Multiferroic memories. *Nat. Mater.* **2007**, *6* (4), 256.
(4) Xiao, Z.; Yuan, Y.; Shao, Y.; Wang, Q.; Dong, Q.; Bi, C.; Sharma, P.; Gruverman, A.; Huang, J. Giant switchable photovoltaic effect in organometal trihalide perovskite devices. *Nat. Mater.* **2015**, *14* (2), 193.
(5) Yang, S.; Seidel, J.; Byrnes, S.; Shafer, P.; Yang, C.-H.; Rossell, M.; Yu, P.; Chu, Y.-H.; Scott, J.; Ager, J., III Above-bandgap voltages from ferroelectric photovoltaic devices. *Nat. Nanotechnol.* **2010**, *5* (2), 143.
(6) Dawber, M.; Rabe, K.; Scott, J. Physics of thin-film ferroelectric oxides. *Rev. Mod. Phys.* **2005**, *77* (4), 1083.
(7) Junquera, J.; Ghosez, P. Critical thickness for ferroelectricity in perovskite ultrathin films. *Nature* **2003**, *422* (6931), 506.
(8) Novoselov, K. S.; Geim, A. K.; Morozov, S. V.; Jiang, D.; Zhang, Y.; Dubonos, S. V.; Grigorieva, I. V.; Firsov, A. A. Electric field effect in atomically thin carbon films. *Science* **2004**, *306* (5696), 666−669.
(9) Kan, E.; Wu, F.; Deng, K.; Tang, W. High-temperature ferroelectricity in two-dimensional atomic crystal. *Appl. Phys. Lett.* **2013**, *103* (19), 193103.
(10) Mehboudi, M.; Dorio, A. M.; Zhu, W.; van der Zande, A.; Churchill, H. O.; Pacheco-Sanjuan, A. A.; Harriss, E. O.; Kumar, P.; Barraza-Lopez, S. Two-dimensional disorder in black phosphorus and monochalcogenide monolayers. *Nano Lett.* **2016**, *16* (3), 1704−1712.
(11) Mehboudi, M.; Fregoso, B. M.; Yang, Y.; Zhu, W.; van der Zande, A.; Ferrer, J.; Bellaiche, L.; Kumar, P.; Barraza-Lopez, S. Structural phase transition and material properties of few-layer monochalcogenides. *Phys. Rev. Lett.* **2016**, *117* (24), 246802.
(12) Barraza-Lopez, S.; Kaloni, T. P.; Poudel, S. P.; Kumar, P. Tuning the ferroelectric-to-paraelectric transition temperature and dipole orientation of group-IV monochalcogenide monolayers. *Phys. Rev. B: Condens. Matter Mater. Phys.* **2018**, *97* (2), 024110.
(13) Shirodkar, S. N.; Waghmare, U. V. Emergence of Ferroelectricity at a Metal-Semiconductor Transition in a 1T Monolayer of MoS_2. *Phys. Rev. Lett.* **2014**, *112* (15), 157601.
(14) Ding, W.; Zhu, J.; Wang, Z.; Gao, Y.; Xiao, D.; Gu, Y.; Zhang, Z.; Zhu, W. Prediction of intrinsic two-dimensional ferroelectrics in In2Se3 and other III_2-VI_3 van der Waals materials. *Nat. Commun.* **2017**, *8*, 14956.
(15) Fei, R.; Kang, W.; Yang, L. Ferroelectricity and Phase Transitions in Monolayer Group-IV Monochalcogenides. *Phys. Rev. Lett.* **2016**, *117* (9), 097601.
(16) Zhang, J.-J.; Lin, L.; Zhang, Y.; Wu, M.; Yakobson, B. I.; Dong, S. Type-II multiferroic $Hf_2VC_2F_2$ MXene monolayer with high transition temperature. *J. Am. Chem. Soc.* **2018**, *140* (30), 9768−9773.
(17) Zheng, C.; Yu, L.; Zhu, L.; Collins, J. L.; Kim, D.; Lou, Y.; Xu, C.; Li, M.; Wei, Z.; Zhang, Y. Room temperature in-plane ferroelectricity in van der Waals In_2Se_3. *Sci. Adv.* **2018**, *4* (7), eaar7720.
(18) Cui, C.; Hu, W.-J.; Yan, X.; Addiego, C.; Gao, W.; Wang, Y.; Wang, Z.; Li, L.; Cheng, Y.; Li, P. Intercorrelated in-plane and out-of-plane ferroelectricity in ultrathin two-dimensional layered semiconductor In_2Se_3. *Nano Lett.* **2018**, *18* (2), 1253−1258.
(19) Chang, K.; Liu, J.; Lin, H.; Wang, N.; Zhao, K.; Zhang, A.; Jin, F.; Zhong, Y.; Hu, X.; Duan, W.; Zhang, Q.; Fu, L.; Xue, Q.-K.; Chen, X.; Ji, S.-H. Discovery of robust in-plane ferroelectricity in atomic-thick SnTe. *Science* **2016**, *353* (6296), 274−278.
(20) Liu, F.; You, L.; Seyler, K. L.; Li, X.; Yu, P.; Lin, J.; Wang, X.; Zhou, J.; Wang, H.; He, H.; Pantelides, S. T.; Zhou, W.; Sharma, P.; Xu, X.; Ajayan, P. M.; Wang, J.; Liu, Z. Room-temperature ferroelectricity in $CuInP_2S_6$ ultrathin flakes. *Nat. Commun.* **2016**, *7*, 12357.
(21) Zhou, Y.; Wu, D.; Zhu, Y.; Cho, Y.; He, Q.; Yang, X.; Herrera, K.; Chu, Z.; Han, Y.; Downer, M. C. Out-of-plane piezoelectricity and ferroelectricity in Layered α-In_2Se_3 nanoflakes. *Nano Lett.* **2017**, *17* (9), 5508−5513.
(22) Hu, T.; Kan, E. Progress and prospects in low-dimensional multiferroic materials. *Wiley Interdisciplinary Reviews: Computational Molecular Science* **2019**, *9*, e1409.
(23) Chang, K.; Kaloni, T. P.; Lin, H.; Bedoya-Pinto, A.; Pandeya, A. K.; Kostanovskiy, I.; Zhao, K.; Zhong, Y.; Hu, X.; Xue, Q. K. Enhanced spontaneous polarization in ultrathin SnTe films with layered antipolar structure. *Adv. Mater.* **2019**, *31* (3), 1804428.
(24) Kaloni, T. P.; Chang, K.; Miller, B. J.; Xue, Q.-K.; Chen, X.; Ji, S.-H.; Parkin, S. S.; Barraza-Lopez, S. From an atomic layer to the bulk: Low-temperature atomistic structure and ferroelectric and electronic properties of SnTe films. *Phys. Rev. B: Condens. Matter Mater. Phys.* **2019**, *99* (13), 134108.
(25) Rørvik, P. M.; Grande, T.; Einarsrud, M. A. One-dimensional nanostructures of ferroelectric perovskites. *Adv. Mater.* **2011**, *23* (35), 4007−4034.
(26) Horiuchi, S.; Tokura, Y. Organic ferroelectrics. *Nat. Mater.* **2008**, *7* (5), 357.
(27) Liang, L.; Kang, X.; Sang, Y.; Liu, H. One-Dimensional Ferroelectric Nanostructures: Synthesis, Properties, and Applications. *Adv. Sci.* **2016**, *3* (7), 1500358.
(28) Tokura, Y.; Koshihara, S.; Iwasa, Y.; Okamoto, H.; Komatsu, T.; Koda, T.; Iwasawa, N.; Saito, G. Domain-wall dynamics in organic charge-transfer compounds with one-dimensional ferroelectricity. *Phys. Rev. Lett.* **1989**, *63* (21), 2405.
(29) Gorshunov, B.; Torgashev, V.; Zhukova, E.; Thomas, V.; Belyanchikov, M.; Kadlec, C.; Kadlec, F.; Savinov, M.; Ostapchuk, T.; Petzelt, J. Incipient ferroelectricity of water molecules confined to nano-channels of beryl. *Nat. Commun.* **2016**, *7*, 12842.
(30) Hernandez, B. A.; Chang, K.-S.; Fisher, E. R.; Dorhout, P. K. Sol− gel template synthesis and characterization of BaTiO3 and PbTiO3 nanotubes. *Chem. Mater.* **2002**, *14* (2), 480−482.
(31) Lasave, J.; Abufager, P.; Koval, S. Ab initio study of the one-dimensional H-bonded ferroelectric CsH_2PO_4. *Phys. Rev. B: Condens. Matter Mater. Phys.* **2016**, *93* (13), 134112.
(32) Shi, L.; Rohringer, P.; Suenaga, K.; Niimi, Y.; Kotakoski, J.; Meyer, J. C.; Peterlik, H.; Wanko, M.; Cahangirov, S.; Rubio, A.; Lapin, Z. J.; Novotny, L.; Ayala, P.; Pichler, T. Confined linear carbon chains as a route to bulk carbyne. *Nat. Mater.* **2016**, *15* (6), 634.
(33) Pham, T.; Oh, S.; Stetz, P.; Onishi, S.; Kisielowski, C.; Cohen, M. L.; Zettl, A. Torsional instability in the single-chain limit of a transition metal trichalcogenide. *Science* **2018**, *361* (6399), 263−266.
(34) Vasylenko, A.; Marks, S.; Wynn, J. M.; Medeiros, P. V.; Ramasse, Q. M.; Morris, A. J.; Sloan, J.; Quigley, D. Electronic Structure Control of Sub-Nanometer 1D SnTe via Nanostructuring within Single-Walled Carbon Nanotubes. *ACS Nano* **2018**, *12* (6), 6023−6031.
(35) Zhao, L.-D.; Lo, S.-H.; Zhang, Y.; Sun, H.; Tan, G.; Uher, C.; Wolverton, C.; Dravid, V. P.; Kanatzidis, M. G. Ultralow thermal conductivity and high thermoelectric figure of merit in SnSe crystals. *Nature* **2014**, *508* (7496), 373.
(36) Kresse, G.; Furthmüller, J. Efficient iterative schemes for ab initio total-energy calculations using a plane-wave basis set. *Phys. Rev. B: Condens. Matter Mater. Phys.* **1996**, *54* (16), 11169.
(37) Kresse, G.; Joubert, D. From ultrasoft pseudopotentials to the projector augmented-wave method. *Phys. Rev. B: Condens. Matter Mater. Phys.* **1999**, *59* (3), 1758.

DOI: 10.1021/jacs.9b03201
J. Am. Chem. Soc. 2019, 141, 15040−15045

(38) Resta, R.; Posternak, M.; Baldereschi, A. Towards a quantum theory of polarization in ferroelectrics: The case of KNbO 3. *Phys. Rev. Lett.* **1993**, *70* (7), 1010.
(39) Resta, R.; Vanderbilt, D. Theory of polarization: a modern approach. *Physics of Ferroelectrics*; Springer, 2007; pp 31−68.
(40) Bruce, A. D. Structural phase transitions. II. Static critical behaviour. *Adv. Phys.* **1980**, *29* (1), 111−217.
(41) Stanley, H. E. *Phase transitions and critical phenomena*; Clarendon Press: Oxford, 1971.
(42) Mermin, N. D.; Wagner, H. Absence of ferromagnetism or antiferromagnetism in one-or two-dimensional isotropic Heisenberg models. *Phys. Rev. Lett.* **1966**, *17* (22), 1133.
(43) Li, X.; Lv, H.; Dai, J.; Ma, L.; Zeng, X. C.; Wu, X.; Yang, J. Half-Metallicity in One-Dimensional Metal Trihydride Molecular Nanowires. *J. Am. Chem. Soc.* **2017**, *139* (18), 6290−6293.
(44) Yang, J.-H.; Zhang, Y.; Yin, W.-J.; Gong, X.; Yakobson, B. I.; Wei, S.-H. Two-dimensional SiS layers with promising electronic and optoelectronic properties: theoretical prediction. *Nano Lett.* **2016**, *16* (2), 1110−1117.
(45) Beleznay, F.; Bogár, F.; Ladik, J. Charge carrier mobility in quasi-one-dimensional systems: Application to a guanine stack. *J. Chem. Phys.* **2003**, *119* (11), 5690−5695.

DOI: 10.1021/jacs.9b03201
J. Am. Chem. Soc. 2019, 141, 15040−15045